Lectin-captured plasma microRNAs predict response and survival in patients with non-small cell lung cancer treated with nivolumab

EIJI NARUSAWA[1*], YUKIKO NAKANO[2*], SESHIRU NAKAZAWA[1], KANJI HORI[2,3], YOICHI OHTAKI[1,4], NATSUKO KAWATANI[1], TOMOHIRO YAZAWA[1], RYOHEI YOSHIKAWA[1], KAZUKI NUMAJIRI[1], RYO KURIYAMA[1], HIROSHI KUROKAWA[2], YOSHIHIRO TAGUCHI[2], SEYED MOSTAFA MOSTAFAVI ZADEH[5], HARUKA OKAMI[5], TAKUYA SHIRAISHI[1], NOBUHIRO NAKAZAWA[1], TAKAMICHI IGARASHI[1], KYOICHI KAIRA[6], HIROSHI SAEKI[1], KEN SHIRABE[1] and TAKEHIKO YOKOBORI[5]

[1]Department of General Surgical Science, Gunma University Graduate School of Medicine, Maebashi, Gunma 371-8511, Japan; [2]The IT Lab Co., Ltd., Morioka, Iwate 020-0857, Japan; [3]Graduate School of Integrated Sciences for Life, Hiroshima University, Higashi-Hiroshima, Hiroshima 739-8528, Japan; [4]Department of Thoracic Surgery, National Cancer Center Hospital East, Kashiwa, Chiba 277-8577, Japan; [5]Division of Gene Therapy Science, Gunma University, Initiative for Advanced Research, Maebashi, Gunma 371-8511, Japan; [6]Department of Respiration Medicine, Saitama Medical University, International Medical Center, Hidaka, Saitama 350-1298, Japan

Received January 23, 2026; Accepted Mach 26, 2026

DOI: 10.3892/ol.2026.15669

Abstract. Predictive biomarkers for response and post-treatment survival of patients with non-small cell lung cancer (NSCLC) treated with immune checkpoint inhibitors (ICIs) are limited. The present study aimed to evaluate whether recombinant *Oscillatoria agardhii* agglutinin (OAA)1-enriched plasma microRNAs (miRNAs/miRs) can serve as predictive and prognostic biomarkers in patients with NSCLC treated with nivolumab. High-mannose glycans, enriched in tumors, were selectively captured using this novel lectin. Pre-treatment plasma samples from 48 patients with NSCLC treated with nivolumab, an ICI, were processed using OAA1 columns. Plasma miRNAs were evaluated for their potential roles as predictive markers of response to nivolumab. The levels of circulating miR-320a, miR-320b and miR-3613-5p, which are associated with nivolumab resistance, were quantified with and without OAA1 enrichment. The three miRNAs were significantly upregulated in patients with stable or progressive disease compared with those with a partial response. For miR-320a, this difference was significant only after OAA1 enrichment. Receiver operating characteristic curve and survival analyses showed improved predictive and prognostic performance for OAA1-enriched miRNAs: The area under the curve for miR-3613-5p improved from 0.837 to 0.897, and the hazard ratio increased from 3.386 to 7.815. In conclusion, OAA1-enriched plasma miRNAs may be associated with resistance to nivolumab and a poor prognosis in NSCLC. This glycan-based enrichment strategy could enhance the clinical value of circulating miRNAs and may complement tissue-based biomarkers of ICI response.

Introduction

Lung cancer is one of the leading causes of cancer-related mortality worldwide, with non-small cell lung cancer (NSCLC) accounting for approximately 80% of all cases (1-3). Immune checkpoint inhibitors (ICIs) that restore antitumor immunity by blocking inhibitory pathways, such as the programmed death-1 (PD-1) and PD-ligand 1 (PD-L1) pathways, have emerged as major therapeutic strategies. In NSCLC, PD-1/PD-L1 blockade enhances T-cell activation and improves patient prognosis (3). Among the ICIs, nivolumab, an anti-PD-1 antibody, has demonstrated clinical efficacy in patients with advanced NSCLC (4). Nevertheless, currently available biomarkers remain inadequate for accurately predicting the sensitivity and clinical outcomes of ICIs, leading to suboptimal patient stratification. Consequently, a substantial proportion of patients do not benefit from treatment and may develop immune-related adverse events or hyperprogression, underscoring the urgent need for reliable predictive biomarkers for advanced NSCLC (5). Several tissue-based markers, such as tumoral PD-L1 expression, tumor mutation burden, and interferon-γ signatures, have been proposed to predict response to ICI and prognosis (3). However, their evaluation requires invasive tumor tissue sampling. Blood-based biomarkers are highly attractive because they can be obtained repeatedly via a minimally

Correspondence to: Professor Takehiko Yokobori, Division of Gene Therapy Science, Gunma University, Initiative for Advanced Research, 3-39-22 Showa-machi, Maebashi, Gunma 371-8511, Japan
E-mail: bori45@gunma-u.ac.jp

*Contributed equally

Key words: miR-320, miR-3613, lung cancer, lectin, immune checkpoint inhibitor

invasive method and may offer a more accurate and dynamic reflection of disease status.

Aberrant glycosylation is a common feature observed in many human malignancies, including NSCLC, and serves as a marker for distinguishing tumor cells from surrounding normal tissues (6). Clinical tumor markers, such as carbohydrate antigen 19-9 and carcinoembryonic antigen, which are widely used in practice to indicate tumor presence and disease progression, reflect cancer-specific glycan structures and are detected in the blood using antibody-based immunoassays (7). Lectins are glycan-binding proteins with high selectivity for specific glycan structures. To distinguish subtle differences in glycan composition, lectins have been widely used in biomarker studies to detect cancer-associated glycan alterations (8). Recent studies have shown that glycosylation of cancer cell surface proteins affects immune evasion and the efficacy of ICIs, highlighting its important role in regulating antitumor immune responses (9).

This study focused on high-mannose glycans, a subclass of tumor-associated glycans that selectively accumulate in certain cancers (10). Notably, a lectibody is a fusion molecule composed of a lectin domain that selectively binds to specific glycan structures and an antibody Fc region that mediates immune effector functions. One such lectibody, constructed by fusing the high-mannose-binding lectin avaren to the human immunoglobulin G1 Fc region, binds specifically to lung cancer cell lines and tumor regions in clinical lung cancer tissues (10). These findings demonstrate the presence of high-mannose glycans in lung cancer cells and the tumor microenvironment.

MicroRNAs (miRNAs) are small non-coding RNAs, 18-25 nucleotides in length, that regulate gene expression by binding to the 3'-untranslated regions of target mRNAs, leading to mRNA degradation or translational repression (11,12). In lung cancer, miR-335, miR-17, miR-146a, and the miR-320 family are candidate regulators of immune checkpoint molecules such as PD-1, PD-L1, CD155, CD28, and cytotoxic T-lymphocyte antigen 4 (13). In this study, we focused on high-mannose glycans, a class of cancer-associated glycan structures, and attempted to identify tumor-specific circulating miR markers by enriching cancer-derived components in the plasma using OAA1, recombinant *Oscillatoria agardhii* agglutinin (OAA), a lectin that selectively binds to high-mannose structures (14,15). Notably, previous studies have reported that miR-320b is significantly upregulated in plasma exosomes from patients with a progressive disease (PD) compared with those with a partial response (PR) at baseline before PD-1/PD-L1 inhibitor treatment (16). Although miR-320a suppresses PD-L1 expression (17), no study has reported an association between its circulating levels and ICI sensitivity in patients with lung cancer. Moreover, to date, no study has demonstrated the involvement of miR-3613-5p in the response to ICIs. Moreover, although lectin-based methods have previously been used to detect and enrich tumor-specific glycan structures in the blood (15), no studies have combined this approach with miRNA profiling to evaluate its potential as a predictive biomarker strategy for response to ICI. Therefore, this study aimed to determine whether OAA1 enrichment of miRNAs could enhance their utility as predictive biomarkers of response to nivolumab treatment and post-treatment survival.

In this study, we developed a novel lectin-based enrichment strategy using an OAA1 lectin column to selectively capture glycan-associated circulating miRNAs from plasma. By combining this approach with circulating miRNA profiling, we aimed to identify biomarkers predictive of response to nivolumab in patients with NSCLC. This strategy enables the enrichment of glycan-associated miRNAs that are not readily detectable using conventional plasma miRNA analyses and may improve the identification of ICI responders and non-responders. Our findings suggest that lectin-captured plasma miRNAs represent a promising and previously unexplored class of predictive biomarkers for immunotherapy response.

Materials and methods

Patients. A total of 48 patients with recurrent or advanced NSCLC who initiated treatment with nivolumab at Gunma University Hospital (Maebashi, Japan), Hidaka Hospital (Takasaki, Japan), and National Hospital Organization Shibukawa Medical Center (Shibukawa, Japan) between February 2016 and November 2017 were included in this study. The inclusion criteria were i) pathologically confirmed NSCLC, ii) recurrent or advanced stage, iii) eligibility for nivolumab treatment following initial chemotherapy, and iv) Eastern Cooperative Oncology Group performance status of 0-2. Plasma samples and clinical data from patients included in a previous study were used (18). Plasma samples from 11 healthy volunteers were used as the controls.

The follow-up period for censored cases ranged from 1.3 to 36.5 months (median: 12.4 months). miRNA microarray analysis was performed using total RNA extracted from OAA1-enriched plasma samples collected before and 1 month post-treatment from two individuals who developed PD despite receiving nivolumab. Patient consent was obtained using the opt-out method. Healthy volunteers were hospital staff aged ≥20 years who provided written informed consent after receiving an explanation of the study. Individuals with a history of malignant disease, acute infection, or regular use of immunosuppressive medications were excluded. Additional exclusion criteria included a bleeding tendency, severe anemia, coagulation disorders, current use of anticoagulant or antiplatelet drugs, pregnancy or breastfeeding, poor physical condition on the day of blood sampling (e.g., fever or presyncope), or any other condition judged inappropriate by the investigators.

This study was conducted in accordance with the Declaration of Helsinki and was approved by the Institutional Review Board for Clinical Research at Gunma University Hospital (Maebashi, Japan; approval no. HS2023-094).

Preparation of OAA1 and OAA1-immobilized column. OAA1, which contained two amino acid substitutions of OAA and an additional linker sequence at the C-terminal region for covalent immobilization, and OAA1-immobilized columns on monolithic silica were prepared according to our previous report (19).

Histochemical analysis of lectin for tumor-specific high-mannose glycans using OAA1. Histochemical analysis

of lectin was performed on formalin-fixed paraffin-embedded sections of lung cancer tissue to detect tumor-specific high-mannose glycans using OAA1. OAA1 was labeled with biotin using the biotin-labeling kit-NH_2 (final concentration: 1.3 mg/ml) [Dojindo Molecular Technologies, Kumamoto, Japan]. Non-specific binding sites were blocked by incubating the sections with 1% bovine serum albumin (Sigma-Aldrich)/phosphate-buffered saline (PBS) for 1 h at room temperature. The sections were then incubated with biotinylated OAA1 diluted in PBS (x800) for 1 h at room temperature. After washing, the slides were treated with the VECTASTAIN Elite ABC Kit (Vector Laboratories, Inc.) for 30 min. The color was developed using a diaminobenzidine (DAB) substrate solution, and the sections were lightly counterstained with hematoxylin and mounted. Negative controls were prepared by omitting the lectin incubation step.

Immunohistochemistry. We obtained 28 sections consisting of resected specimens (n=20) and needle biopsies (n=8) from patients for whom clinical samples were obtained.

For immunohistochemistry, 4-μm sections were cut from the paraffin blocks of each sample. Each section was mounted on a silane-coated glass slide, deparaffinized in xylene, rehydrated through graded ethanol to water, and incubated with 0.3% hydrogen peroxide for 30 min at room temperature to block endogenous peroxidase activity. After rehydration through a graded series of the ethanol treatments (90% for 1 min, 80% for 1 min, and 60% for 1 min), the sections for CD8 staining were heated in boiling water using Immunosaver (Nisshin EM Co., Ltd.) for 45 min at 98-100˚C for antigen retrieval. For PD-L1 staining, Universal HIER antigen retrieval reagent (cat. no. ab208572; Abcam) at 120˚C for 20 min in an autoclave. Non-specific binding sites were blocked by incubating the sections with Protein Block Serum-Free (Agilent Technologies) for 30 min at room temperature. Samples were incubated overnight at 4˚C with the following primary antibodies: PD-L1 (E1L3N Rabbit mAb 1:200; cat. no. 13684; Cell Signaling Technology, Inc., Danvers, MA) and CD8 (cat. no. ab4055; 1:1,000; Abcam). The primary antibody was visualized using the Histofine Simple Stain MAX-PO (Multi) Kit (Nichirei Biosciences, Inc.). Chromogen 3,3-diaminobenzidine tetrahydrochloride was used as a 0.02% solution in 50 mM citric acid-ammonium acetate buffer (pH 6) containing 0.005% hydrogen peroxide. The sections were lightly counterstained with hematoxylin and mounted.

Tissue sections were examined by two independent evaluators who were blinded to the patient data. The expression of PD-L1 was evaluated using a semiquantitative scoring method based on the percentage of stained cells: 1, ≤1; 2, 1-5; 3, 5-10; 4, 10-50; and 5, ≥50%. Tumors with a score >3 were graded as positive. CD8 expression was semi-quantitatively evaluated based on the extent of positive lymphocyte infiltration in the tumor specimens, and patients with >5% positive lymphocytes were defined as positive, based on previous studies (20-22).

MicroRNA extraction from OAA1-captured plasma samples. To enrich for tumor-specific high-mannose glycan-containing molecules, plasma samples were subjected to lectin affinity capture using an OAA1 column. OAA1 was immobilized on a silica monolith matrix in the column. Briefly, each plasma sample was centrifuged at 10,000 x g for 10 min, and 50 μl of plasma was applied onto the pre-equilibrated OAA1 column. The column was centrifuged at 3,000 x g for 1 min to allow the sample to pass through. After binding, unbound plasma components were removed by washing the column with 400 μl of 10X D-PBS (-) (FUJIFILM Wako Pure Chemical Corporation) and D-PBS (-) (FUJIFILM Wako Pure Chemical Corporation). Glycan-containing molecules specifically bound to OAA1 were then eluted using 200 μl of QIAzol Lysis Reagent (QIAGEN), which was applied to a column and allowed to stand for 5 min at room temperature by centrifugation at 3,000 x g for 1 min.

Total RNA, including miRNA, was extracted from glycan-containing molecules in the plasma samples as follows: 40 μl of chloroform was added to each sample, and the tubes were shaken vigorously for 15 sec. The tubes were incubated at room temperature for 2 min, followed by centrifugation at 12,000 x g for 5 min. The upper aqueous phase was carefully transferred to a new tube, and an equal volume of isopropanol was added. After thorough vortex mixing, the miRNA was purified using the NucleoSpin miRNA Plasma kit (Macherey-Nagel, Germany) with DNA digestion treatment, according to the manufacturer's protocol. Without the OAA1 enrichment group, miRNA was directly extracted from plasma samples using the NucleoSpin miRNA Plasma kit with DNA digestion treatment, according to the manufacturer's protocol. The concentration and purity of the extracted RNA were assessed using a NanoDrop spectrophotometer (Thermo Fisher Scientific), and miRNA samples were stored at -80˚C until further analysis. The amount of RNA obtained from the plasma-derived, lectin-captured fraction was extremely low and consisted primarily of short RNAs such as miRNAs; therefore, reliable quantification using NanoDrop and quality assessment based on the RNA integrity number were difficult. In this study, RNA was extracted from 50 μl of plasma from each sample, and RNA quality was indirectly evaluated based on the reproducibility and stability of Ct values in the TaqMan miRNA assay.

miRNA microarray. For miRNA microarray analysis, to enrich tumor-specific high-mannose glycan-containing molecules, plasma samples were subjected to lectin affinity capture using OAA1 lectin columns, as previously described, with modifications to the sample volume and extraction protocol. Briefly, 1 ml of plasma was divided equally among five OAA1 columns (200 μl plasma per column), each containing OAA1 immobilized on a silica monolith matrix. After centrifugation of each plasma sample at 10,000 x g for 10 min, the plasma was applied to pre-equilibrated columns. The columns were centrifuged at 3,000 x g for 1 min to allow the samples to pass through. After washing, glycan-containing molecules bound to OAA1 were eluted by adding 200 μl of QIAzol Lysis Reagent to each column and incubating at room temperature for 5 min, followed by centrifugation at 3,000 x g for 1 min. The eluates from each column were combined, and total RNA, including miRNA, was extracted as follows: chloroform was added to the QIAzol eluate, and the mixture was vigorously vortexed. After phase separation, the upper aqueous phase was collected, and an equal volume of isopropanol was added. miRNA was purified using the NucleoSpin miRNA Plasma kit with DNA

digestion treatment, according to the manufacturer's protocol, for subsequent miRNA microarray analysis.

Microarray analysis was performed using the GeneChip™ miRNA 4.0 Array (Thermo Fisher Scientific). RNA labeling was performed with the FlashTag™ Biotin HSR RNA Labeling Kit (Thermo Fisher Scientific) according to the manufacturer's protocol, with a minor modification: instead of adjusting the RNA input based on concentration, the maximum recommended sample volume (8 μl per sample) was used, due to variability in RNA yield from the upstream lectin-based procedure. Subsequent steps, including hybridization, washing, staining, and scanning, were performed according to the manufacturer's instructions.

miRNA microarray analysis and candidate selection (discovery phase). miRNA microarray analysis was conducted as an exploratory discovery step. Only miRNAs classified as 'T' (true detection) by the microarray analysis software were included, whereas those flagged as 'F' (not reliably detected) were excluded from subsequent analyses. Candidate miRNAs were selected based on differential abundance between paired pre-treatment and post-treatment plasma samples from the same patients.

miRNAs exhibiting a fold change >2 and a nominal P-value <0.05 were considered eligible for further validation. To minimize potential sex-related bias, miRNAs encoded on sex chromosomes (X or Y) were excluded from candidate selection.

Reverse transcription-quantitative polymerase chain reaction (RT-qPCR) for miRNA. For miR-320a (assay ID 002277), miR-320b (assay ID 002844), and miR-3613-5p (assay ID 463197_mat; Thermo Fisher Scientific), RT-qPCR was performed, and cDNA was synthesized from total miRNA using the TaqMan™ MicroRNA Reverse Transcription Kit (Thermo Fisher Scientific) and specific stem-loop reverse transcription primers (Thermo Fisher Scientific) according to the manufacturer's protocol. The exact primer and probe sequences used in the TaqMan MicroRNA Assays are proprietary and were not disclosed by the manufacturer; therefore, the assay identification numbers are provided to ensure reproducibility. The 15 μl reaction volumes were incubated in 0.2 ml tubes, and the following temperature profile was used: 16˚C for 30 min, followed by 42˚C for 30 min, and 85˚C for 5 min. PCR was performed using a QuantStudio™ 5 System (Thermo Fisher Scientific). The 10 μl PCR mix, including the TaqMan™ Fast Advanced Master Mix for RT-qPCR (Thermo Fisher Scientific), was incubated in a 384-well optical plate at 95˚C for 20 s, followed by 40 cycles of 95˚C for 1 sec and 60˚C for 20 sec. Levels of miR-320a, miR-320b, and miR-3613-5p were normalized to that of miR-16-5p (used as an internal control; assay ID 000391) and analyzed using the $2^{-\Delta Cq}$ method. miR-16-5p was chosen as a suitable reference gene, as described previously (23-25). The fold change in target miRNA expression relative to that in healthy volunteers was determined using the $2^{-\Delta\Delta Cq}$ method (26,27).

Statistical analysis. Statistical analyses were performed using the Mann-Whitney U test for continuous variables and χ^2 test or Fisher's exact test for categorical variables. ROC curve analysis was performed to compare the prognostic utility of OAA1-captured plasma miRNAs with that of plasma miRNAs without OAA1 treatment. Kaplan-Meier curves were generated for overall survival, and statistical significance was examined using the log-rank test. Univariate analyses were performed using logistic regression or the Cox proportional hazards model. $P<0.05$ was considered to indicate a statistically significant difference. All statistical analyses were performed using IBM SPSS Statistics, version 31 (IBM Corp., Armonk, NY) and GraphPad Prism version 10 (GraphPad Software, San Diego, CA). Figures were generated using GraphPad Prism version 10.

The Cancer Genome Atlas (TCGA) data analysis using UALCAN. TCGA RNA-seq data were analyzed using the UALCAN web portal (http://ualcan.path.uab.edu). For lung adenocarcinoma and lung squamous cell carcinoma cohorts, mRNA expression levels (transcripts per million) of N-glycan biosynthesis and processing enzymes, including ALG3 α-1,3-mannosyltransferase (ALG3), mannosidase α class 1A member 1 (MAN1A1), mannosidase α class 1C member 1 (MAN1C1), α-1,3-mannosyl-glycoprotein 2-β-N-acetylglucosaminyltransferase (MGAT1) and β-1,4-mannosyl-glycoprotein 4-β-N-acetylglucosaminyltransferase (MGAT3), were retrieved and compared between primary tumor and normal tissues using TCGA module of UALCAN. Statistical significance of expression differences was assessed using an unpaired two sample t-test implemented in UALCAN.

Results

Identification of circulating OAA1-captured miRs associated with lung cancer and resistance to nivolumab. Fig. 1A shows the histochemical results for OAA1 in surgically resected lung cancer specimens. This analysis revealed that high-mannose glycan structures bound by OAA1 were more abundantly expressed in lung cancer cells than in adjacent non-tumorous tissues (Fig. 1A). Similarly, TCGA RNA-seq data analysis via UALCAN showed a higher expression of ALG3, with an early addition of mannose during N-glycan assembly in the endoplasmic reticulum, and lower expression of mannosidase MAN1A1 and MAN1C1, resulting in trimmed mannose residues in the Golgi to prepare glycans for further processing, as well as lower expression of MGAT1, which initiates complex N-glycan branching with the addition of GlcNAc, and MGAT3, resulting in a 'bisecting' GlcNAc that modulates later branching (28-30). These expression patterns were consistent with the attenuated trimming and maturation of N-glycans in tumors (Figs. S1 and S2).

Based on this finding, we used OAA1 to selectively capture glycan-containing molecules associated with tumors from the plasma of patients with lung cancer and conducted miRNA microarray analysis to identify circulating miRNAs that were elevated during treatment in patients who exhibited tumor progression to PD despite nivolumab therapy (Fig. 1B). As shown in Fig. 1C, several candidate miRNAs were identified. Among them, hsa-miR-320a, hsa-miR-320b, and hsa-miR-3613-5p were significantly upregulated in OAA1-captured plasma samples after treatment compared with their pre-treatment levels. Furthermore, we quantified these OAA1-captured miRNAs in pre-treatment plasma

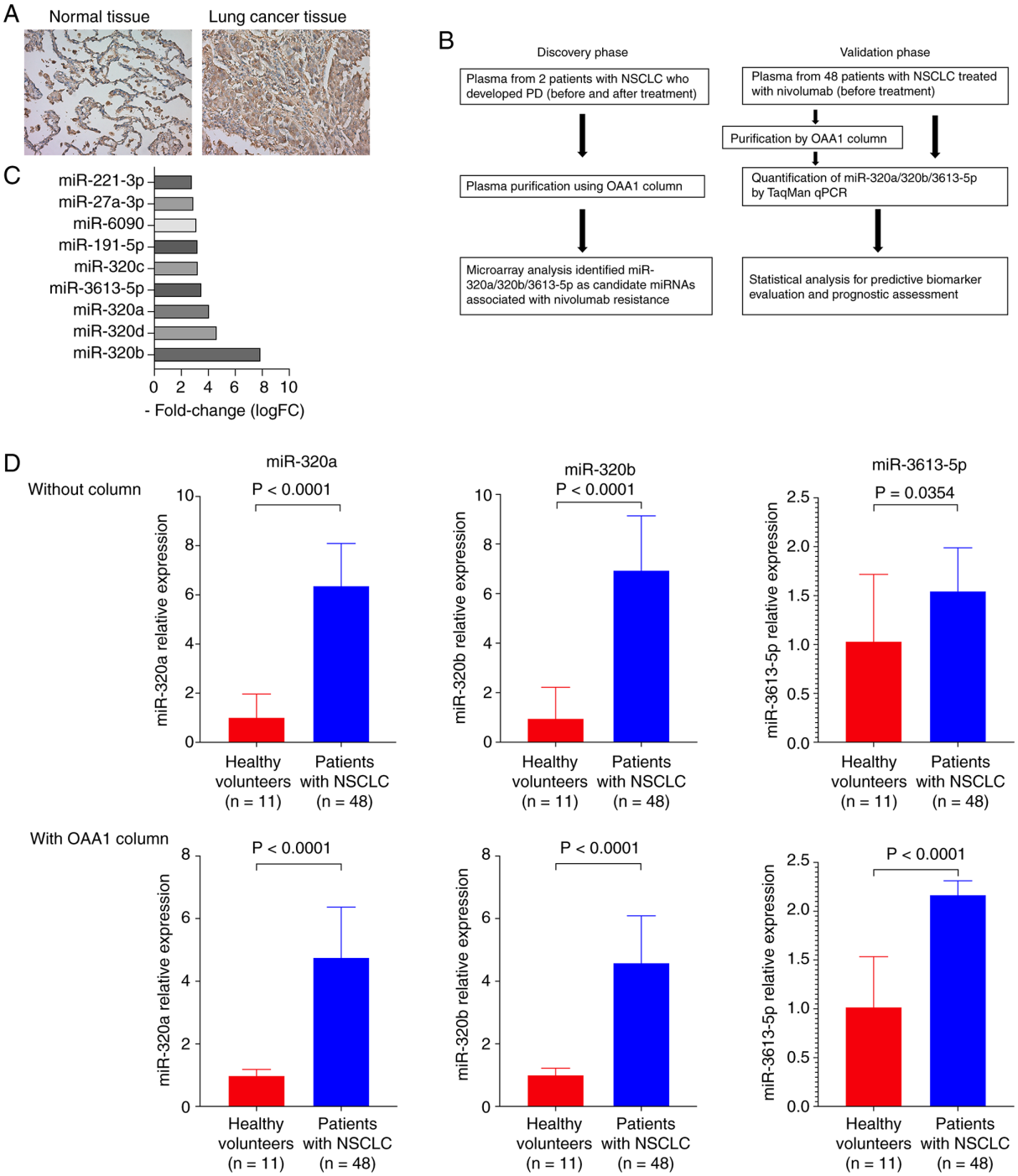

Figure 1. Identification of circulating OAA1-captured miRNAs associated with lung cancer and resistance to nivolumab. (A) Lectin histochemistry using OAA1 on surgically resected lung cancer tissues (x200 magnification). The left panel shows OAA1 lectin staining in normal lung tissue, whereas the right panel shows OAA1 lectin staining in lung cancer tissue. (B) In the discovery phase, plasma samples from two patients with NSCLC with PD were collected before and after nivolumab treatment. After plasma purification using an OAA1 column, microarray analysis was performed to identify candidate miRNAs (miR-320a, miR-320b, and miR-3613-5p) associated with nivolumab resistance. In the validation phase, plasma samples from 48 patients with NSCLC (before nivolumab treatment) were analyzed with and without OAA1 column purification. The levels of the identified miRNAs were quantified using TaqMan qPCR, and statistical analyses were conducted to evaluate their predictive and prognostic values as biomarkers for nivolumab resistance. (C) Microarray analysis of OAA1-captured plasma miRNAs in patients with PD after nivolumab treatment reveals several upregulated candidate miRNAs, including miR-320a, miR-320b, and miR-3613-5p. (D) Relative levels of miR-320a, miR-320b, and miR-3613-5p in pre-treatment plasma from patients with NSCLC (n=48) and healthy controls (n=11) with and without OAA1 enrichment. Plasma miRNA levels were quantified by reverse transcription-qPCR. Relative miRNA levels were normalized to miR-16-5p and calculated using the $2^{-\Delta\Delta Cq}$ method, with the mean level of healthy volunteers serving as the calibrator. Statistical significance was determined using the Mann-Whitney U test. Data are presented as median with 95% confidence intervals. miRNA/miR, microRNA; NSCLC, non-small cell lung cancer; OAA1, *Oscillatoria agardhii* agglutinin 1; PD, progressive disease; qPCR, quantitative polymerase chain reaction.

samples from patients with advanced or recurrent NSCLC (n=48) and healthy volunteers (n=11). As shown in Fig. 1D, the levels of these miRNAs were significantly higher in patients with NSCLC than in healthy controls.

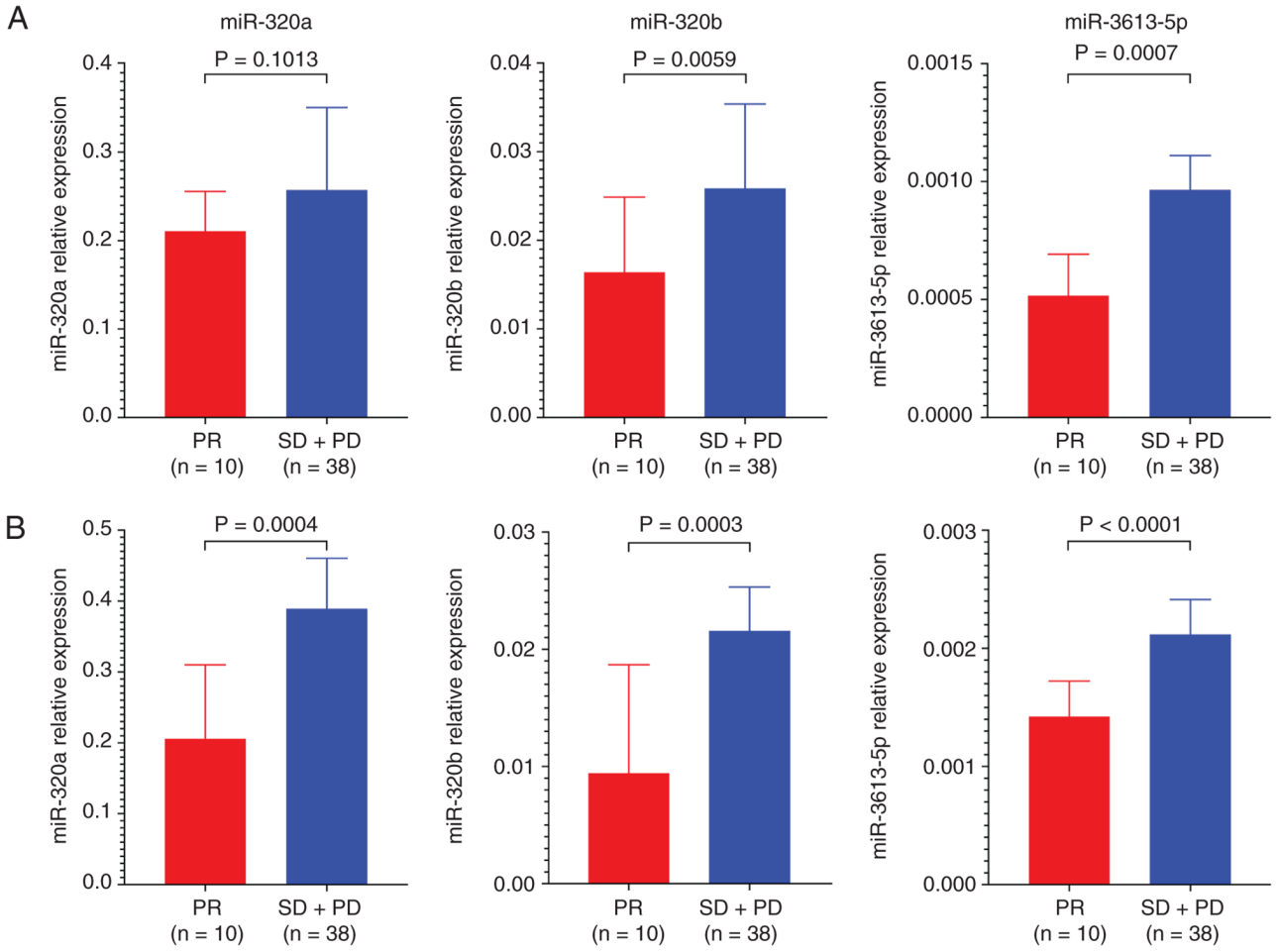

Figure 2. Differential expression of miR-320a, miR-320b, and miR-3613-5p in pre-treatment plasma from patients with non-small cell lung cancer with PR or SD + PD. (A) Relative levels of miR-320a, miR-320b, and miR-3613-5p without OAA1 enrichment. (B) With OAA1 column enrichment. Plasma miRNA levels were quantified by reverse transcription-quantitative polymerase chain reaction and are shown as relative abundance using the $2^{-\Delta Cq}$ method normalized to miR-16-5p. Statistical significance was determined using the Mann-Whitney U test. Data are presented as median with 95% confidence intervals. miR, microRNA; OAA1, *Oscillatoria agardhii* agglutinin 1; SD, stable disease; PD, progressive disease; PR, partial response.

Differential expression of miR-320a, miR-320b, and miR-3613-5p with and without OAA1 enrichment in the plasma samples of patients with PR vs. those with stable disease (SD) + PD. Next, we measured the levels of miR-320a, miR-320b, and miR-3613-5p in plasma samples collected before nivolumab treatment from patients who exhibited PR (n=10) and SD + PD (n=38). This analysis was conducted under two conditions: With and without OAA1 enrichment. Without OAA1 enrichment, there was no significant difference in the levels of miR-320a between the PR and SD + PD groups. However, both miR-320b and miR-3613-5p were expressed at significantly higher levels in the SD + PD group than in the PR group (Fig. 2 A). In contrast, with OAA1 enrichment, the levels of all three miRNAs (miR-320a, miR-320b, and miR-3613-5p) were significantly higher in the SD + PD group than in the PR group (Fig. 2 B), suggesting that OAA1 enrichment enhances the sensitivity of circulating miRNA-based detection for predicting the response to nivolumab.

OAA1 enrichment enhances the predictive power of circulating miRNAs for response to nivolumab in NSCLC. Univariate logistic regression analysis was performed to evaluate the association between circulating miRNA levels and response to nivolumab (SD or PD) in patients with NSCLC (Table I). Without OAA1 enrichment, the odds ratios for predicting SD/PD were 3.208 for miR-320a, 12.444 for miR-320b, and 19.5 for miR-3613-5p. In contrast, with OAA1 enrichment, the odds ratios increased to 12.889 for miR-320a, 27.222 for miR-320b, and 39.857 for miR-3613-5p, representing a substantial improvement compared with the values obtained without OAA1 enrichment (Table I). These results suggest that OAA1 enrichment improves the predictive utility of circulating miRNAs for identifying patients with poor response to nivolumab. This finding is consistent with an earlier comparison between the PR and SD + PD groups and supports the potential of OAA1-captured plasma miRNAs as predictive biomarkers in NSCLC.

OAA1 enrichment enhances the predictive accuracy of circulating miRNAs for response to nivolumab in patients with NSCLC. To evaluate the prognostic value of circulating miR-320a, miR-320b, and miR-3613-5p in patients who responded to nivolumab, receiver operating characteristic (ROC) curve analyses were performed with and without OAA1 enrichment. Without OAA1 enrichment, the area under the curve (AUC) values for miR-320a, miR-320b,

Table I. Univariate logistic regression analysis of clinicopathological factors and circulating pre-treatment miRNA levels for predicting SD + PD.

Clinicopathological characteristic	Odds ratio (95% confidence interval)	P-value
Age, years		
≤65	1	0.331
>65	2.100 (0.471-9.364)	
Sex		
Male	1	0.942
Female	1.067 (0.188-6.045)	
Histology		
SQC	1	0.395
ADC	0.481 (0.089-2.601)	
Recurrent disease		
Negative	1	1
Positive	1 (0.248-4.03)	
Levels of tumor markers		
Low	1	0.686
High	0.745 (0.179-3.096)	
PD-L1 status		
Negative	1	0.658
Positive	0.658 (0.131-3.610)	
CD8 expression		
Negative	1	0.374
Positive	0.350 (0.035-3.548)	
Levels of miR-320a		
Low	1	0.127
High	3.208 (0.717-14.35)	
Levels of OAA1 captured miR-320a		
Low	1	0.004[a]
High	12.889 (2.307-72.02)	
Levels of miR-320b		
Low	1	0.002[a]
High	12.444 (2.489-62.21)	
Levels of OAA1 captured miR-320b		
Low	1	<0.001[a]
High	27.222 (4.53-163.75)	
Levels of miR-3613-5p		
Low	1	0.007[a]
High	19.50 (2.213-171.86)	
Levels of OAA1 captured miR-3613-5p		
Low	1	0.001[a]
High	39.857 (4.317-368.02)	

[a]P<0.05. ADC, adenocarcinoma; miR, microRNA; OAA1, *Oscillatoria agardhii* agglutinin 1; PD-L1, programmed death ligand 1; PR, partial response; SD + PD, stable or progressive disease; SQC, squamous cell carcinoma.

and miR-3613-5p were 0.671 [95% confidence interval (CI): 0.502-0.840], 0.779 (95% CI: 0.632-0.926) and 0.837 (95% CI: 0.722-0.952), respectively (Fig. 3A). In contrast, with OAA1 enrichment, the AUCs increased to 0.847 (95% CI: 0.723-0.967) for miR-320a, 0.853 (0.718-0.988) for miR-320b, and 0.897 (95% CI: 0.807-0.987) for miR-3613-5p, showing improved performance compared with the corresponding values obtained without OAA1 enrichment (Fig. 3B). These results suggest that OAA1 enrichment improves the prognostic performance of these circulating miRNAs for overall survival in patients with NSCLC treated with nivolumab.

The optimal cutoff values ($2^{-\Delta Cq}$) were determined using the ROC analysis. Without OAA1 enrichment, the cutoff values were 0.2335 for miR-320a, 0.01662 for miR-320b, and 6.947×10^{-4} for miR-3613-5p, whereas with OAA1 enrichment, the corresponding values were 0.2610, 0.01164, and 1.740×10^{-3}, respectively.

Association between OAA1-enriched circulating miRNAs and survival outcomes in patients with NSCLC treated with nivolumab. Circulating miRNA profiles with and without OAA1 enrichment were categorized into high- and low-expression groups based on the cutoff values determined by the ROC curves for patients who responded to nivolumab, as shown in Fig. 3. Based on each ROC-based threshold, 48 patients with NSCLC were stratified into high or low miRNA expression groups. Table SI summarizes the association between the levels of the target miRNAs and clinicopathological features without OAA1 enrichment. In the group without OAA1, high levels of miR-320b and miR-3613-5p were significantly associated with low sensitivity to nivolumab (SD and PD); however, no other clinical features were significantly correlated (Table SI). In contrast, with OAA1 enrichment, a high expression of all three target miRNAs was significantly associated with SD and PD (Table SII).

Kaplan-Meier survival analysis with log-rank testing was performed to assess the prognostic relevance of circulating miR-320a, miR-320b, and miR-3613-5p in patients with NSCLC treated with nivolumab with and without OAA1 enrichment. High plasma levels of these miRNAs were significantly associated with poor overall survival, regardless of the OAA1 enrichment status (Fig. 4).

Cox regression analysis was used to evaluate the prognostic relevance of circulating miRNA levels for overall survival in patients with NSCLC based on univariate modeling (Table II). Without OAA1 enrichment, the hazard ratios (HRs) for predicting poor survival were 2.136 for miR-320a, 3.578 for miR-320b, and 3.386 for miR-3613-5p. In contrast, with OAA1 enrichment, the corresponding HRs increased to 2.389 for miR-320a, 7.922 for miR-320b, and 7.815 for miR-3613-5p (Table II). These results indicate that OAA1 enrichment enhances the prognostic utility of circulating miRNAs and improves their ability to stratify patients according to overall survival following nivolumab treatment. Multivariable Cox regression analysis, including CD8 expression and the miRNAs identified as significant in the univariate analysis, further supported these findings. In the analysis without OAA1 enrichment, CD8 expression (P=0.008, HR=0.149), miR-320b (P=0.024, HR=5.505) and miR-3613-5p (P=0.048, HR=3.152) were identified as independent prognostic factors.

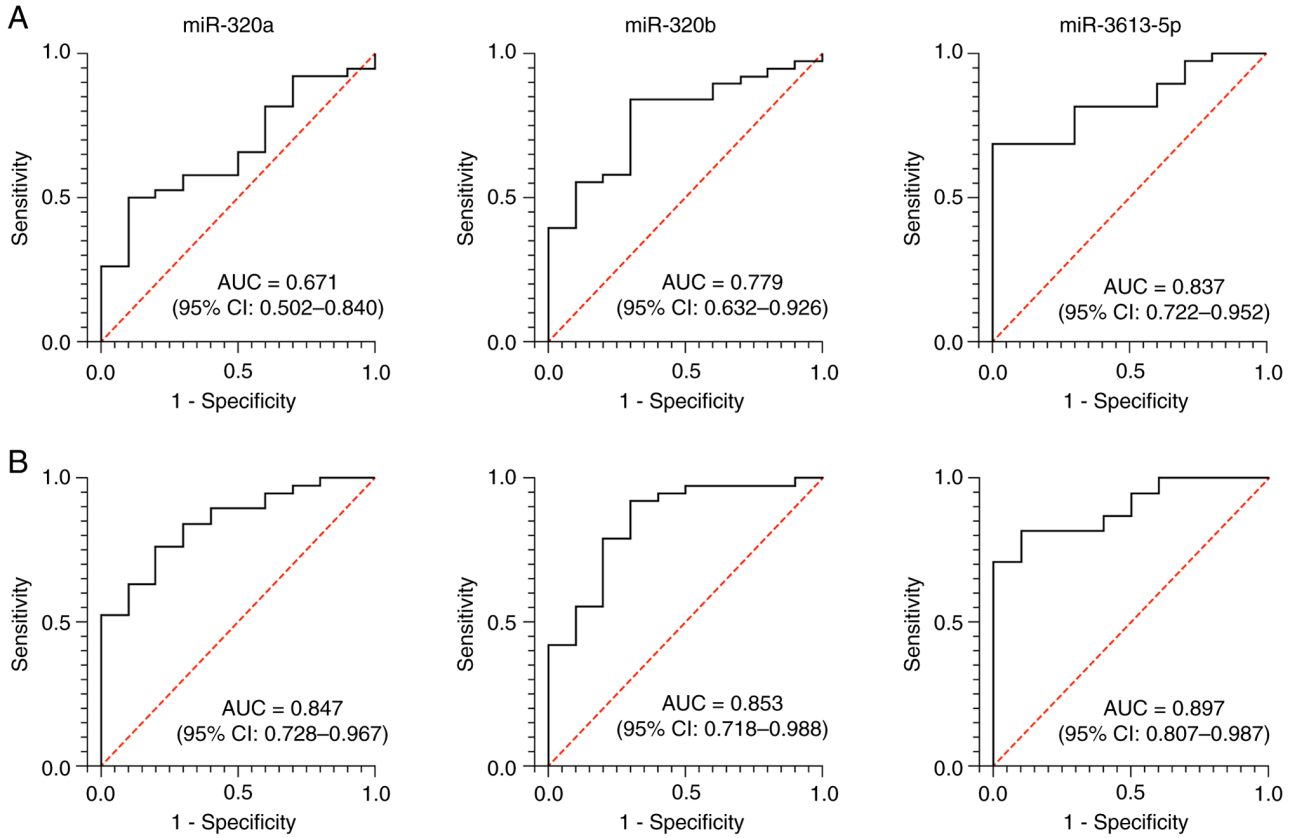

Figure 3. ROC curve analysis of miRNAs for predicting non-response to immune checkpoint inhibitor therapy in patients with non-small cell lung cancer treated with nivolumab. (A) ROC curves for circulating miR-320a, miR-320b, and miR-3613-5p without OAA1 column enrichment. (B) With OAA1 enrichment. AUC, area under the curve; CI, confidence interval; miR, microRNA; OAA1, *Oscillatoria agardhii* agglutinin 1; ROC, receiver operating characteristic.

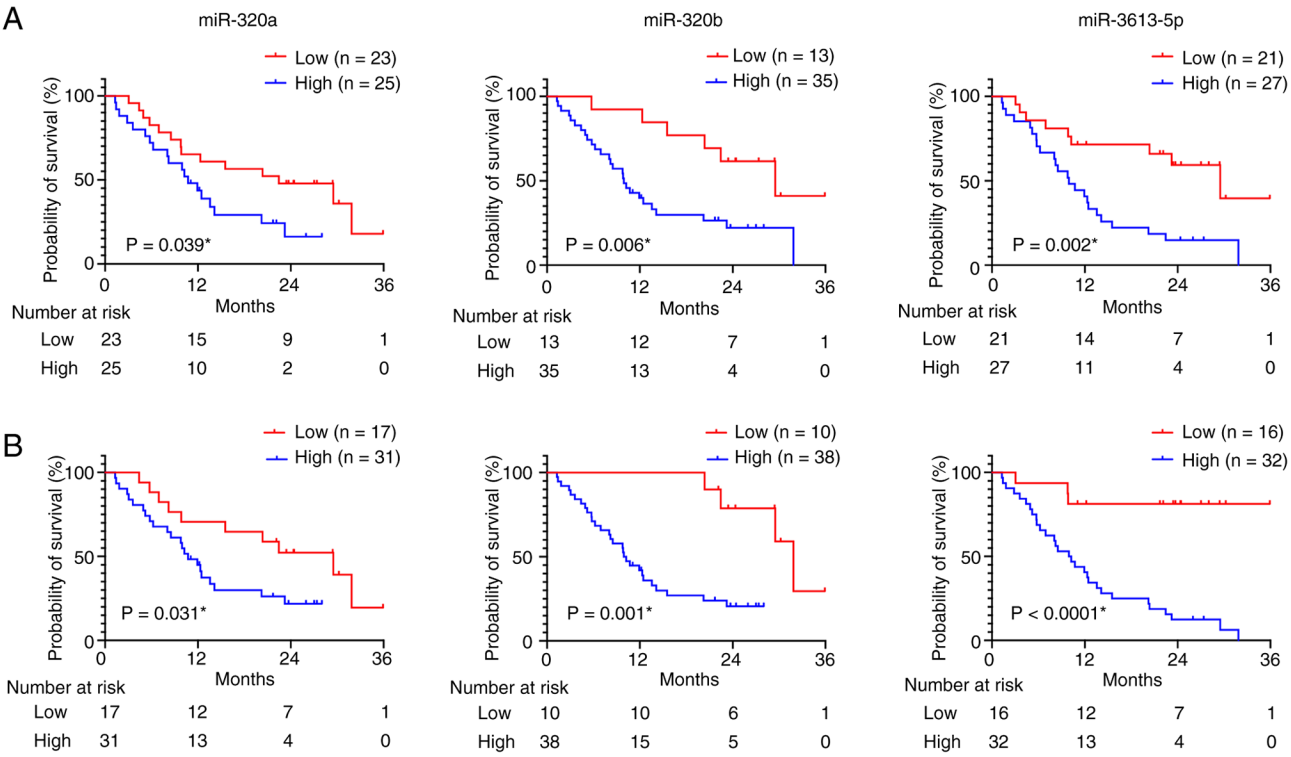

Figure 4. Kaplan-Meier analysis for OS based on pre-treatment plasma levels of miR-320a, miR-320b, and miR-3613-5p in patients with non-small cell lung cancer treated with nivolumab (n=48). (A) Kaplan-Meier curves comparing the OS between the high- and low-expression groups for each miRNA without OAA1 column enrichment. (B) Kaplan-Meier curves for the same miRNAs with the OAA1 enrichment. The number of patients in each group is indicated in the legends. Cutoff values for high/low expression were determined using receiver operating characteristic analysis. P-values are shown; *P<0.05. miR, microRNA; OAA1, *Oscillatoria agardhii* agglutinin 1; OS, overall survival.

Table II. Univariate Cox regression analysis of clinicopathological factors and circulating pre-treatment miRNA levels of patients with non-small cell lung cancer treated with nivolumab.

Clinicopathological characteristic	Hazard ratio (95% confidence interval)	P-value
Age, years		
≤65	1	0.787
>65	0.908 (0.448-1.837)	
Sex		
Male	1	0.33
Female	1.224 (0.815-1.838)	
Smoking		
No	1	0.385
Yes	1.238 (0.767-2.004)	
Histology		
SQC	1	0.7
ADC	0.929 (0.637-1.354)	
Recurrent disease		
Negative	1	0.587
Positive	0.822 (0.406-1.666)	
PD-L1 status		
Negative	1	0.725
Positive	0.827 (0.286-2.388)	
CD8 expression		
Negative	1	0.026[a]
Positive	0.283 (0.094-0.858)	
Levels of tumor markers		
Low	1	0.185
High	1.634 (0.791-3.377)	
Levels of miR-320a		
Low	1	0.043[a]
High	2.136 (1.022-4.461)	
Levels of OAA1 captured miR-320a		
Low	1	0.036[a]
High	2.389 (1.059-5.390)	
Levels of miR-320b		
Low	1	0.01[a]
High	3.578 (1.357-9.435)	
Levels of OAA1 captured miR-320b		
Low	1	0.005[a]
High	7.922 (1.868-33.59)	
Levels of miR-3613-5p		
Low	1	0.003[a]
High	3.386 (1.499-7.649)	
Levels of OAA1 captured miR-3613-5p		
Low	1	<0.001[a]
High	7.815 (2.359-25.89)	

[a]P<0.05. ADC, adenocarcinoma; miR, microRNA; OAA1, *Oscillatoria agardhii* agglutinin 1; PD-L1, programmed death ligand 1; PR, partial response; SD + PD, stable or progressive disease; SQC, squamous cell carcinoma.

In contrast, in the analysis with OAA1 enrichment, only miR-3613-5p remained an independent prognostic factor (P=0.010, HR=7.462) (Tables SIII and SIV). Notably, the HR of miR-3613-5p was higher with OAA1 enrichment than without enrichment.

Discussion

In this study, we identified circulating miR-320a, miR-320b, and miR-3613-5p as miRNAs that were upregulated after treatment compared with pre-treatment levels in the plasma of patients with NSCLC with PD despite nivolumab therapy. We further demonstrated that these miRNAs were significantly associated with disease progression and poor prognosis in patients with NSCLC treated with nivolumab. Histochemical analysis of lectin using OAA1 showed that high-mannose glycan structures were abundantly expressed in lung cancer tissues compared with adjacent non-tumorous areas.

Supporting the presence of high-mannose-type glycans indicated by lectin staining, gene expression analysis of the TCGA lung cancer cohort using the UALCAN database (http://ualcan.path.uab.edu) also revealed characteristic changes in glycan enzyme expression. Specifically, in lung cancer tissues, the expression of the high-mannose-type glycosyltransferase ALG3 was significantly elevated compared with that in normal lung tissues. Conversely, the expression of Golgi α-mannosidases I (MAN1A1 and MAN1C1), which are responsible for removing and processing high-mannose-type N-glycans, and N-acetylglucosamine transferases (MGAT1 and MGAT3) was significantly reduced [Figs. S1 and S2] (28). MGAT1 initiates the conversion of high-mannose to hybrid/complex N-glycans, whereas MGAT3 adds bisecting GlcNAc, which modulates branching. The reduced expression of these enzymes is expected to impair maturation and favor the retention of high-mannose glycans (29). Indeed, a relative increase in N-glycans with high-mannose structures has been reported in the tissues of patients with lung cancer compared with normal tissues, which is consistent with the gene expression patterns revealed in this analysis (30). These results provide molecular-level support for the possibility that high-mannose-type glycans are produced and accumulate due to abnormalities in the glycan synthesis pathway in tumor cells.

In addition, extracellular vesicles (EVs) reflect the molecular characteristics of their cells of origin, including glycosylation patterns. Therefore, EVs released from tumor cells with aberrant glycan biosynthesis are expected to carry high-mannose-type glycans on their surface. Consistent with this notion, the OAA1 lectin column selectively captured EV-associated particles bearing high-mannose glycans, as evidenced by the enrichment of EV markers and tumor-associated miRNAs in the captured fraction (19). Overall, these findings support the interpretation that a substantial proportion of the lectin-captured EVs originate from tumor cells and retain tumor-specific glycosylation features.

Based on this finding, we established a strategy to selectively enrich tumor-derived glycan-associated molecules from plasma using an OAA1 lectin column, followed by miRNA profiling. Circulating miRNAs captured by OAA1

showed significantly higher expression in patients with SD or PD than in those with PR. Logistic regression analysis revealed that the odds ratios for predicting SD/PD were markedly increased in the OAA1-enrichment group, indicating an improved predictive power. Furthermore, ROC curve and Kaplan-Meier analyses showed that high expression of these miRNAs was significantly associated with poor overall survival, regardless of OAA1 enrichment status. Notably, both AUC and HRs consistently improved with OAA1 enrichment, further indicating its prognostic performance. To the best of our knowledge, this is the first study to demonstrate that plasma enrichment of tumor-specific glycans using lectin combined with circulating miRNA profiling improves the prediction of resistance to ICIs and poor prognosis in NSCLC.

In addition to OAA1, several other lectins that bind high-mannose-type glycans, such as Concanavalin A (ConA), *Galanthus nivalis* lectin (GNL), and *Narcissus pseudonarcissus* agglutinin (NPA), have long been used in glycomic analyses and cancer biomarker studies. However, these lectins generally exhibit broad binding affinities for high-mannose and other glycans that may be present in non-tumor tissues, thereby limiting their tumor specificity (8). In contrast, OAA, a novel lectin derived from the cyanobacterium *Oscillatoria agardhii*, selectively recognizes and binds to high-mannose structures present in tumor cell-derived exosomes (15). OAA1 (a recombinant OAA) shows minimal binding to secreted factors derived from noncancerous cells and exhibits a unique capacity to enrich tumor-specific components (19). In addition to its high specificity and strong binding affinity, OAA exhibits remarkable physicochemical stability. Previous studies have demonstrated that its activity is maintained over a wide pH range (pH 4-11) and under high-temperature conditions (31). Furthermore, its activity is independent of divalent cations, as neither EDTA treatment nor the addition of Ca^{2+}, Mg^{2+}, or Mn^{2+} affects its function. Based on these characteristics and the specific binding of OAA1 to tumor cells, we considered OAA1 to be superior to other mannose-binding lectins for selectively enriching tumor-associated glycans with miRNA biomarkers. Therefore, we employed OAA1 in this study to identify predictive markers of nivolumab sensitivity.

The association between high levels of circulating miR-320a, miR-320b, and miR-3613-5p with poor response to nivolumab in patients with NSCLC suggests that these miRNAs may be involved in the mechanisms of immune evasion or resistance to PD-1 blockade. Previous studies have reported that members of the miR-320 family suppress PD-L1 expression and modulate T-cell activation and cytokine signaling by regulating immune checkpoint molecules (13). In contrast, although high levels of PD-L1 protein expression in tumor tissues are generally associated with poor prognosis (32), tumors that simultaneously exhibit abundant CD8+ cytotoxic T-cell infiltration are considered 'hot tumors' and are well known to respond favorably to ICI therapy (33). Particularly, miR-320 family members target PD-L1 mRNA, promoting its degradation and thereby reducing PD-L1 protein levels. Therefore, in our cohort with high plasma levels of miR-320a and miR-320b, it is plausible that the intratumoral expression of these miRNAs leads to the suppression of PD-L1 protein, thereby shifting the immune landscape toward a 'cold tumor' phenotype with reduced immunogenicity and ICI sensitivity. Although miR-320a has been reported to function as a tumor suppressor in NSCLC by inhibiting tumor cell proliferation and invasion (34,35), its immunomodulatory effects, particularly PD-L1 suppression, may paradoxically contribute to an immune-cold tumor microenvironment with limited responsiveness to immune checkpoint blockade.

Furthermore, a recent study on immune reconstitution after allogeneic hematopoietic stem cell transplantation in patients with acute myeloid leukemia reported that elevated plasma levels of miR-3613-5p were inversely correlated with the number of peripheral CD8+ cytotoxic T cells (36). This suggests that miR-3613-5p may reflect systemic immunosuppression. Collectively, these findings indicate that high levels of circulating miRNAs may mark a tumor microenvironment characterized by low PD-L1 expression and impaired CD8+ T-cell activity, which is consistent with a cold tumor state. Such patients may be unable to mount an effective immune response despite nivolumab administration, resulting in therapeutic resistance and a poor prognosis. Therefore, the OAA1-based plasma miRNA assay may serve as a noninvasive tool for assessing the immune status of nivolumab-targeted lesions. In our cohort, we observed no correlation between PD-L1 and miRNA levels. This null finding may reflect limited PD-L1 availability (assessed in only 28 of 48 patients) and temporal discordance because PD-L1 was measured in archival surgical or biopsy specimens rather than immediately before nivolumab initiation. Further studies are warranted to investigate the relationship between OAA1-captured circulating miRNAs and the intratumoral expression of immune checkpoint proteins and immune cell infiltration.

The evaluation of circulating miRNAs captured from the plasma using OAA1 holds promise as a blood-based biomarker for predicting therapeutic responses and stratifying prognosis in the context of ICI treatment, particularly in patients with NSCLC. Although current biomarkers, such as PD-L1 expression and tumor mutational burden, are widely used to guide ICI therapy (6), they are tissue-based and thus limited by their invasiveness and challenges associated with repeated assessment. The strategy investigated in this study, which involves the enrichment of cancer-derived glycans from plasma using OAA1, followed by miRNA quantification, provides a minimally invasive and repeatable alternative. This approach may be particularly useful in cases where tumor tissue is difficult to obtain or where longitudinal monitoring during treatment is necessary. Importantly, the identified miRNAs were associated with nivolumab sensitivity and clinical outcomes, highlighting their potential as biomarkers for treatment selection and disease monitoring in patients with advanced NSCLC. Taken together, these OAA1-based assays may complement existing tissue-derived markers and support personalized approaches for ICI therapy.

This study had some limitations. First, the relatively small sample size might have limited the statistical power to detect significant associations. In addition, the cutoff values used to classify miRNA levels into high and low groups were derived from ROC analysis based on nivolumab response status. However, validation in large independent external cohorts

is required to ensure the generalizability of these findings. Second, PD-L1 and CD8 immunohistochemistry could only be evaluated in 28 of the 48 patients because of the limited availability of tissue samples. This partial ascertainment may introduce a selection bias and limit the statistical power, and the combination of resected specimens and needle biopsies may also increase sampling variability.

Third, although the enrichment of plasma components using OAA1 improved the performance of miRNA biomarkers, the underlying biological mechanisms remain unclear. The coexistence of high-mannose glycans with miRNAs and their contribution to nivolumab sensitivity and patient prognosis remain unclear. Finally, the analysis was limited to patients with NSCLC who were treated with nivolumab. Therefore, it remains uncertain whether the identified miRNAs or the OAA1-based enrichment method is applicable to other ICIs or different tumor types. In addition, because the amount of RNA obtained from the plasma-derived, lectin-captured fraction was extremely low, spectrophotometric RNA quality assessment using NanoDrop was performed near the lower detection limit of the instrument, making it difficult to obtain reliable absorbance spectra or purity ratios. Therefore, in this study, RNA quality was primarily evaluated based on the stability and reproducibility of Ct values of the endogenous control miRNA (miR-16-5p), as measured using the TaqMan miRNA assay.

In conclusion, this study identified circulating miR-320a, miR-320b, and miR-3613-5p as promising biomarkers of nivolumab resistance and poor prognosis in NSCLC. By employing the tumor-specific high-mannose glycan-binding lectin OAA1, we successfully established a novel strategy to capture and enrich glycan-associated molecules from the plasma. This approach enables a more sensitive detection of clinically relevant miRNAs and improves their predictive and prognostic performance. The consistent enhancement of AUCs, odds ratios, and HRs following OAA1-based enrichment highlights the utility of glycan-focused sample processing in liquid biopsy strategies. Importantly, this is the first study to demonstrate that lectin-mediated glycan capture can augment the clinical value of circulating miRNAs in ICI therapy. These findings offer a promising foundation for developing precise oncology tools that integrate glycomics and miRNA-based profiling to optimize therapeutic decision-making in NSCLC and other malignancies.

Acknowledgements

The authors would like to thank Ms. Mariko Nakamura (Department of General Surgical Science, Graduate School of Medicine, Maebashi, Gunma, Japan), Ms. Kao Abe (Division of Gene Therapy Science, Gunma University, Initiative for Advanced Research, Maebashi, Gunma, Japan) and Ms. Yukiko Suto (Core Facility Management and Technical Collaboration Center, Maebashi, Gunma, Japan) for technical and administrative assistance.

Funding

This study was supported by Grants-in-Aid for Scientific Research from the Japan Society for the Promotion of Science (JSPS; grant no. 23K08288); the Japan Agency for Medical Research and Development (AMED; grant no. JP256f0137008); the Gunma Foundation for Medicine and Health Science Research; and the Takeda Science Foundation.

Availability of data and materials

The miRNA microarray data generated in the present study may be found in the Gene Expression Omnibus under accession number GSE310370 or at the following URL: https://www.ncbi.nlm.nih.gov/geo/query/acc.cgi?acc=GSE310370. The other data generated in the present study may be requested from the corresponding author.

Authors' contributions

EN, YN, SN and TYo contributed to the study concept and design. EN was responsible for data and statistical analyses, and drafting and revision of the manuscript. YN performed sample processing, data collection, data interpretation, and drafting and revision of the manuscript. KS and HS contributed to data analysis and interpretation, and assisted in the preparation of the manuscript. KH, YO, NK, TYa, RY, KN, RK, HK, YT, SMMZ, HO, TS, NN, TI and KK contributed to data collection, analysis and interpretation, and critically reviewed the manuscript. EN, YN and TYo confirm the authenticity of all the raw data. All authors read and approved the final manuscript.

Ethics approval and consent to participate

The present study was conducted in accordance with The Declaration of Helsinki and was approved by the Institutional Review Board for Clinical Research at Gunma University Hospital (Maebashi, Japan; approval no. HS2023-094). Informed consent to participate was obtained from patients using an opt-out method. Written informed consent for participation in this study was obtained from all the healthy volunteers.

Patient consent for publication

Not applicable.

Competing interests

YO, NK, TYa, RY, KN, RK, SMMZ, HO, TS, NN, TI, KK, HS and KS declare no competing interests. EN, YN, SN, KH, HK, YT, KS, and TYo are co-inventors on a pending patent application related to a lectin-column formulation and its applications, titled 'Method for Predicting Response to Immune Checkpoint Inhibitor Therapy and Kit' (filed September 11, 2025). The patent applicant (assignee) is The IT Lab Co., Ltd. KH and HK are employees, YN is an employee and shareholder, and YT is a co-founder and board member of The IT Lab Co., Ltd. TYo received research grants from The IT Lab. Co., Ltd., which also provided the study materials.

References

1. Bray F, Laversanne M, Sung H, Ferlay J, Siegel RL, Soerjomataram I and Jemal A: Global cancer statistics 2022: GLOBOCAN estimates of incidence and mortality worldwide for 36 cancers in 185 countries. CA Cancer J Clin 74: 229-263, 2024.

2. Siegel RL, Kratzer TB, Giaquinto AN, Sung H and Jemal A: Cancer statistics, 2025. CA Cancer J Clin 75: 10-45, 2025.
3. Zhang J, Song Z, Zhang Y, Zhang C, Xue Q, Zhang G and Tan F: Recent advances in biomarkers for predicting the efficacy of immunotherapy in non-small cell lung cancer. Front Immunol 16: 1554871, 2025.
4. Brahmer JR, Lee JS, Ciuleanu TE, Bernabe Caro R, Nishio M, Urban L, Audigier-Valette C, Lupinacci L, Sangha R, Pluzanski A, *et al*: Five-year survival outcomes with nivolumab plus ipilimumab versus chemotherapy as first-line treatment for metastatic non-small-cell lung cancer in CheckMate 227. J Clin Oncol 41: 1200-1212, 2023.
5. Li Y, Chen T, Nie TY, Han J, He Y, Tang X and Zhang L: Hyperprogressive disease in non-small cell lung cancer after PD-1/PD-L1 inhibitors immunotherapy: Underlying killer. Front Immunol 14: 1200875, 2023.
6. Giurini EF, Pappas SG and Gupta KH: Sweet surprises: Decoding tumor-associated glycosylation in cancer progression and therapeutic potential. Cells 15: 233, 2026.
7. Lee T, Teng TZJ and Shelat VG: Carbohydrate antigen 19-9-tumor marker: Past, present, and future. World J Gastrointest Surg 12: 468-490, 2020.
8. Islam MK, Khan M, Gidwani K, Witwer KW, Lamminmäki U and Leivo J: Lectins as potential tools for cancer biomarker discovery from extracellular vesicles. Biomark Res 11: 85, 2023.
9. Ren X, Lin S, Guan F and Kang H: Glycosylation targeting: A paradigm shift in cancer immunotherapy. Int J Biol Sci 20: 2607-2621, 2024.
10. Oh YJ, Dent MW, Freels AR, Zhou Q, Lebrilla CB, Merchant ML and Matoba N: Antitumor activity of a lectibody targeting cancer-associated high-mannose glycans. Mol Ther 30: 1523-1535, 2022.
11. Valencia-Sanchez MA, Liu J, Hannon GJ and Parker R: Control of translation and mRNA degradation by miRNAs and siRNAs. Genes Dev 20: 515-524, 2006.
12. Smolarz B, Durczyński A, Romanowicz H, Szyłło K and Hogendorf P: miRNAs in cancer (review of literature). Int J Mol Sci 23: 2805, 2022.
13. Cánovas-Cervera I, Nacher-Sendra E, Suay G, Lahoz A, García-Giménez JL and Mena-Mollá S: Role of miRNAs as epigenetic regulators of immune checkpoints in lung cancer immunity. Int Rev Cell Mol Biol 390: 109-139, 2025.
14. Sato Y, Okuyama S and Hori K: Primary structure and carbohydrate binding specificity of a potent anti-HIV lectin isolated from the filamentous cyanobacterium Oscillatoria agardhii. J Biol Chem 282: 11021-11029, 2007.
15. Yamamoto M, Harada Y, Suzuki T, Fukushige T, Yamakuchi M, Kanekura T, Dohmae N, Hori K and Maruyama I: Application of high-mannose-type glycan-specific lectin from Oscillatoria agardhii for affinity isolation of tumor-derived extracellular vesicles. Anal Biochem 580: 21-29, 2019.
16. Peng XX, Yu R, Wu X, Wu SY, Pi C, Chen ZH, Zhang XC, Gao CY, Shao YW, Liu L, *et al*: Correlation of plasma exosomal microRNAs with the efficacy of immunotherapy in EGFR/ALK wild-type advanced non-small cell lung cancer. J Immunother Cancer 8: e000376, 2020.
17. Costa C, Indovina P, Mattioli E, Forte IM, Iannuzzi CA, Luzzi L, Bellan C, De Summa S, Bucci E, Di Marzo D, *et al*: P53-regulated miR-320a targets PDL1 and is downregulated in malignant mesothelioma. Cell Death Dis 11: 748, 2020.
18. Yokobori T, Yazawa S, Asao T, Nakazawa N, Mogi A, Sano R, Kuwano H, Kaira K and Shirabe K: Fucosylated α1-acid glycoprotein as a biomarker to predict prognosis following tumor immunotherapy of patients with lung cancer. Sci Rep 9: 14503, 2019.
19. Nakayama S, Umeda M, Kobayashi K, Nakano Y, Hori K, Umemura T and Kurokawa H: MicroRNAs in circulating extracellular vesicles as biomarkers of early colorectal cancer captured using high-mannose N-glycan-specific lectin from Oscillatoria agardhii. Front Oncol 15: 1619460, 2025.
20. Nakazawa N, Yokobori T, Kaira K, Turtoi A, Baatar S, Gombodorj N, Handa T, Tsukagoshi M, Ubukata Y, Kimura A, *et al*: High stromal TGFBI in lung cancer and intratumoral CD8-positive T cells were associated with poor prognosis and therapeutic resistance to immune checkpoint inhibitors. Ann Surg Oncol 27: 933-942, 2020.
21. Kuriyama K, Yokobori T, Sohda M, Nakazawa N, Yajima T, Naruse I, Kuwano H, Shirabe K, Kaira K and Saeki H: Plasma Plastin-3: A tumor marker in patients with non-small-cell lung cancer treated with nivolumab. Oncol Lett 21: 11, 2021.
22. Kaira K, Higuchi T, Naruse I, Arisaka Y, Tokue A, Altan B, Suda S, Mogi A, Shimizu K, Sunaga N, *et al*: Metabolic activity by 18F-FDG-PET/CT is predictive of early response after nivolumab in previously treated NSCLC. Eur J Nucl Med Mol Imaging 45: 56-66, 2018.
23. Yoruker EE, Terzioglu D, Teksoz S, Uslu FE, Gezer U and Dalay N: MicroRNA expression profiles in papillary thyroid carcinoma, benign thyroid nodules and healthy controls. J Cancer 7: 803-809, 2016.
24. McDermott AM, Kerin MJ and Miller N: Identification and validation of miRNAs as endogenous controls for RQ-PCR in blood specimens for breast cancer studies. PLoS One 8: e83718, 2013.
25. Dezfuli NK, Alipoor SD, Dalil Roofchayee N, Seyfi S, Salimi B, Adcock IM and Mortaz E: Evaluation expression of miR-146a and miR-155 in non-small-cell lung cancer patients. Front Oncol 11: 715677, 2021.
26. Schmittgen TD and Livak KJ: Analyzing real-time PCR data by the comparative C(T) method. Nat Protoc 3: 1101-1108, 2008.
27. Monastirioti A, Papadaki C, Kalapanida D, Rounis K, Michaelidou K, Papadaki MA, Mavroudis D and Agelaki S: Plasma-based microRNA expression analysis in advanced stage NSCLC patients treated with nivolumab. Cancers (Basel) 14: 4739, 2022.
28. Chatterjee S, Ugonotti J, Lee LY, Everest-Dass A, Kawahara R and Thaysen-Andersen M: Trends in oligomannosylation and α1,2-mannosidase expression in human cancers. Oncotarget 12: 2188-2205, 2021.
29. Ruhaak LR, Taylor SL, Stroble C, Nguyen UT, Parker EA, Song T, Lebrilla CB, Rom WN, Pass H, Kim K, *et al*: Differential N-glycosylation patterns in lung adenocarcinoma tissue. J Proteome Res 14: 4538-4549, 2015.
30. Lattova E, Skrickova J, Hausnerova J, Krystofova K, Zdrahal Z, Kren L and Popovic M: N-glycans in lung tissue specimens: A prospective target for enhanced cancer diagnosis and prognosis. J Transl Med 23: 918, 2025.
31. Sato Y, Murakami M, Miyazawa K and Hori K: Purification and characterization of a novel lectin from a freshwater cyanobacterium, Oscillatoria agardhii. Comp Biochem Physiol B Biochem Mol Biol 125: 169-177, 2000.
32. Wang A, Wang HY, Liu Y, Zhao MC, Zhang HJ, Lu ZY, Fang YC, Chen XF and Liu GT: The prognostic value of PD-L1 expression for non-small cell lung cancer patients: A meta-analysis. Eur J Surg Oncol 41: 450-456, 2015.
33. Tumeh PC, Harview CL, Yearley JH, Shintaku IP, Taylor EJM, Robert L, Chmielowski B, Spasic M, Henry G, Ciobanu V, *et al*: PD-1 blockade induces responses by inhibiting adaptive immune resistance. Nature 515: 568-571, 2014.
34. Khandelwal A, Sharma U, Barwal TS, Seam RK, Gupta M, Rana MK, Vasquez KM and Jain A: Circulating miR-320a acts as a tumor suppressor and prognostic factor in non-small cell lung cancer. Front Oncol 11: 645475, 2021.
35. Yadav R, Khatkar R, Yap KC, Kang CY, Lyu J, Singh RK, Mandal S, Mohanta A, Lam HY, Okina E, *et al*: The miRNA and PD-1/PD-L1 signaling axis: An arsenal of immunotherapeutic targets against lung cancer. Cell Death Discov 10: 414, 2024.
36. Izadifard M, Ahmadvand M, Chahardouli B, Vaezi M, Janbabai G, Seghatoleslami G, Bahrami M, Yaghmaie M and Barkhordar M: Plasma-circulating miR-638, miR-6511b-5p, miR-3613-5p, miR-455-3p, miR-5787, and miR-548a-3p as noninvasive biomarkers of immune reconstitution post-allogeneic hematopoietic stem cell transplantation in acute myeloid leukemia patients. Transpl Immunol 91: 102240, 2025.